EVOLUTIONARY BIOLOGY

The trilobite upper limb branch is a well-developed gill

Jin-bo Hou[1]*, Nigel C. Hughes[1,2], Melanie J. Hopkins[3]

Whether the upper limb branch of Paleozoic "biramous" arthropods, including trilobites, served a respiratory function has been much debated. Here, new imaging of the trilobite *Triarthrus eatoni* shows that dumbbell-shaped filaments in the upper limb branch are morphologically comparable with gill structures in crustaceans that aerate the hemolymph. In *Olenoides serratus*, the upper limb's partial articulation to the body via an extended arthrodial membrane is morphologically comparable to the junction of the respiratory book gill of *Limulus* and differentiates it from the typically robust exopod junction in Chelicerata or Crustacea. Apparently limited mechanical rotation of the upper branch may have protected the respiratory structures. Partial attachment of the upper branch to the body wall may represent an intermediate state in the evolution of limb branch fusion between dorsal attachment to the body wall, as in Radiodonta, and ventral fusion to the limb base, as in extant Euarthropoda.

INTRODUCTION

Early metazoan diversification was coincident with important ecological and environmental changes, such as increased trophic complexity and metazoan mobility, and rising ambient oxygen availability (*1*–*3*). How increasing energetic demands were accommodated anatomically among early metazoans remains unclear. Our understanding of nonskeletal form in fossil organisms is limited to sites of exceptional preservation (Lagerstätten) (*4*–*7*), from which Paleozoic arthropod soft tissue preservation provides an opportunity to assess structural innovation among soft tissues. However, debate remains about the interpretation of such soft tissues, such as whether the upper branch of the earliest "biramous" limbs was respiratory or not (*8*–*14*).

The Paleozoic biramous appendage consists of an upper branch and a lower branch, similar to the modern arthropod biramous appendage that is composed of a nonrespiratory outer exopod and an inner endopod. The apparent similarity between the Paleozoic biramous appendage and the modern biramous limb (e.g., Anaspidacea) suggests the possible homology of these two sets of structures (*11*, *12*, *15*, *16*). At least one cell lineage study, however, suggests that the modern biramous limb of crustaceans formed via a subdivision of the main proximal-distal limb axis (*17*), and this might not have been the case in the Paleozoic biramous appendage (*18*). Thus, it may be that the two branches seen in many Paleozoic arthropods are not homologous with the modern limb but are rather a uniramous walking leg with an associated exite that evolved into the upper branch but was originally an additional axis (*17*) as in stem lineage arthropods, such as Radiodonta (*19*, *20*). Resolving this issue requires better understanding of the detailed anatomy of the upper branch.

Trilobites are a well-defined clade of Paleozoic arthropods (*21*), but only two species, the corynexochid *Olenoides serratus* from the Cambrian Burgess Shale and the olenid *Triarthrus eatoni* from the Ordovician Beecher's Beds, are sufficiently well preserved to provide information relevant to this analysis, and both are routinely used in phylogenetic analyses of early arthropods (*22*, *23*). Critically, the Burgess Shale and Beecher's Beds Lagerstätten are characterized by different modes of preservation, and while each preserves anatomical features not normally captured in the fossil record, neither preserves organisms with complete fidelity. Thus, some features observable on specimens from one locality may not be observable from specimens at the other locality, even if they had been present when the organisms were alive. Nonetheless, by applying diverse imaging technologies, we are able to report structural details of the upper limb branch of both trilobite species that indicate its respiratory function and also bear on arthropod limb evolution.

RESULTS

Outstandingly well-preserved material shows that the shaft of the upper branch in *T. eatoni* is segmented and composed of annulation-like articles (figs. S1, A and D, and S2, A to C). It tapers distally with a terminal, elongate spoon-like article similar to the filaments that are attached to the articles (Fig. 1A and figs. S1A and S2, A to C). The filaments are reduced in length along the proximal-distal axis of the branch (figs. S1A and S2, A and B). The longest filament is about 3.5 times the length of the distal article, and the shortest filament is almost one-third of the length of the distal article (fig. S2, A and B). When viewed from the rear of the animal, cross sections of the filaments show inflated bulbs at the top and bottom that are connected via a narrow central region to form a dumbbell shape (Figs. 1, A to I, and 2, A to V, and figs. S1, A to F, S3, A to N, S4, A to C, S5, A to D, S6D, and S7, A to D). Measured at the thickest part, the marginal bulbs are about 31 to 49 μm in width, and the narrow central region is about 15 to 26 μm in width. The interval between adjacent marginal bulbs is about 15 to 28 μm wide. The inflated marginal bulb grades into the narrow central region without distinct boundary, and the whole of the inflated marginal bulb is wider than the central region (Figs. 1, A to I, and 2, A to V, and figs. S1, A to C, S3, A to N, S6D, and S7, A to D). Inflated marginal bulbs are commonly well preserved, while the central regions are generally less so (figs. S1, D to F, S2C, S4, A to C, S5, A to D, and S6, C and E).

The limb base, the most proximal unit of the lower branch of *O. serratus*, is a subrectangular structure, the length of which is about 1.3 times its width (Fig. 3, A, C, and D to I, and fig. S8, A to C). Gnathobasic spines are present along its ventral and inner margins (Fig. 3, C, D, and F to H, and fig. S8, A and B). Spines on the inner margin are smaller than those on the ventral margin (*8*). The

[1]Department of Earth and Planetary Sciences, University of California, Riverside, CA 92521, USA. [2]Geological Studies Unit, Indian Statistical Institute, Kolkata 700108, India. [3]Division of Paleontology (Invertebrates), American Museum of Natural History, New York, NY 10024, USA.
*Corresponding author. Email: jhou006@ucr.edu

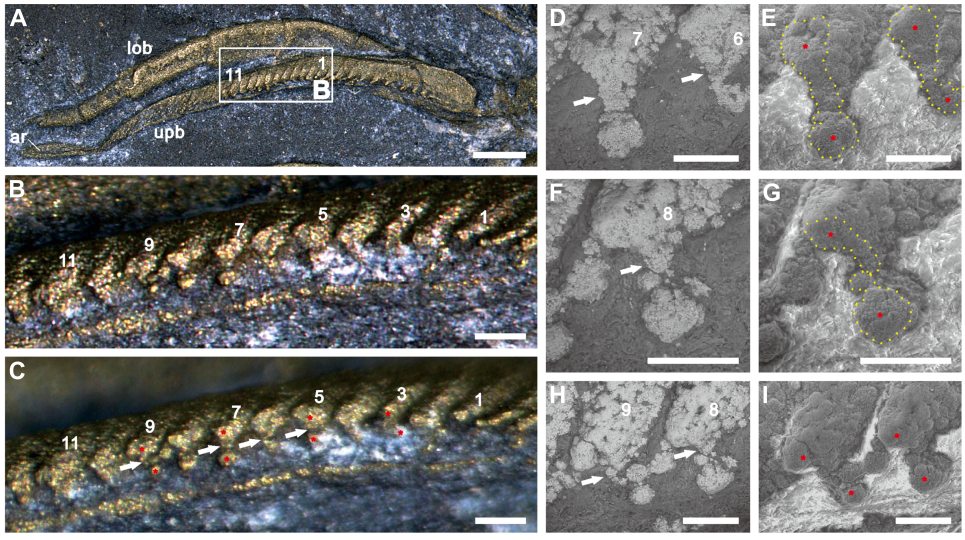

Fig. 1. Dumbbell-shaped filaments of *T. eatoni*. (**A** to **I**) YPM 204 (part). (A) Dorsal view. (B) Posterior view of the truncated filaments in stacked (A). (C) Same area of (B) with nonstack function. (D and E) The sixth and seventh filaments showing dumbbell-shaped outline, tilted about 40° to the dorsal view. (D) High-contrast backscattered electron (BSE) image. (E) High-contrast, gaseous secondary electron (GSE) image. (F and **G**) The eighth filament showing dumbbell-shaped outline, tilted about 40° to the dorsal view. (F) BSE image. (G) GSE image. (H and I) Top view of the eighth and ninth filaments showing dumbbell-shaped outlines. (H) BSE image. (I) GSE image. Yellow dotted lines mark the cross section of the filaments (E and G). Arabic numbers are references for locating the cross section of filaments in (A). Asterisks locate the top and bottom inflated marginal bulbs of dumbbell-shaped filaments. Small white arrows indicate the narrow central region of dumbbell-shaped filament. The BSE image distinguishes bright filament from dark surrounding matrix. The GSE image distinguishes dark filament from bright surrounding matrix. ar, article of shaft; lob, lower branch of the limb; upb, upper branch of the limb. Scale bars, 500 μm (A), 100 μm (B and C), and 50 μm (D to I).

upper limb branch has two lobes, of which the proximal lobe bears long filaments on its posterior and inner margins (Fig. 3, A to I, and fig. S8, A to C). The filaments on the inner margin extend up to the innermost edge of the proximal lobe (Fig. 3, D, F, G, I, and J) but not beyond. The dorsal inner region of the upper branch connects with the lateral body wall and the ventral sternite via the arthrodial membrane. This type of attachment is similar to the oblique limb articulation (*24*), in which the limb joins the body where both lateral and ventral body walls connect. Arcuate, inosculating wrinkle-like structures give a rippled relief to the convex areas to which the proximal limb attached (Fig. 3, A to J, and fig. S8, A to C) and can be distinguished from the blade-like gill filaments that have sharp, straight boundaries (Fig. 3, C, D, and G to I, and fig. S8, A to C). Similar structures are also preserved in other early arthropods, including *Arthroaspis bergstroemi* (*23*), *Misszhouia longicaudata* (*25*), *Waptia fieldensis* (*26*), and *Leanchoilia illecebrosa* (*27*), and interpreted as extended arthrodial membrane with high flexibility. Together, the upper branch, lower branch, and inner region with wrinkle-like structures form a triangular-to-subcircular area (Fig. 3, A to J, and fig. S8, A to C) that marks the body-limb junction. The part of the limb joined to the body wall is about two-fifths of the dorsal width of the entire limb base.

Isolated biramous limbs are commonly preserved detached from the main body (*25*, *28*). Not only does their preservation show the strong connection between the limb base and the proximal portion of the upper branch along a rigid hinge (Fig. 3, A to J, and fig. S8, A to C), but some detached limbs also show the proximal part of the upper branch with arthrodial membrane still attached (Fig. 3, F and G).

In dorsal view, the upper limb branches in both *T. eatoni* and *O. serratus* are distinctly overlapped above the lower limb branches (figs. S2, A to E, and S8, A and C). Two types of imbrication can be recognized in dorsal view when an animal faces anteriorly and its dorsal side is uppermost: anterior imbrication style in which anterior structures cover posterior ones and posterior imbrication style in which posterior structures cover anterior ones. For the lower branch, anterior imbrication characterizes the cephalic region, while posterior imbrication dominates the trunk region (figs. S2B and S8A). This is because, during preservation, cephalic limbs generally rotated forward, overlapping those behind them, while the posterior ones rotated backward (figs. S2, A and B, and S8A). The upper branches show anterior imbrication only, suggesting limited ability to rotate the limb in the narrow space between the lower branch and the dorsal exoskeleton (figs. S2, A to E, and S8, A to C). The upper branches have limited rotation compared to the lower branches, and their range of movement was thus likely impeded.

DISCUSSION

Dumbbell-shaped filament

An inflated marginal bulb is characteristic of crustacean gills, especially in those of decapods (fig. S9, A to E). It provides mechanical support for the respiratory lamellae, guides hemolymph circulation (*29*, *30*), and may help keep the lamellae apart during gas exchange (*31*). In some modern crustaceans, the cuticle of the marginal bulb is thick relative to that of the inner filament region where respiratory exchange takes place. The filament of the upper branch of *T. eatoni* with its inflated marginal bulbs and narrow central region mimics that seen in the gill in decapods. We posit that the inflated marginal bulbs supported the filament and provided channels for hemolymph circulation and that the narrow central region was used in gas exchange (Fig. 4A). The inflated marginal bulbs may also have provided the additional function of maintaining space between adjacent lamellae similar to the knobs or nodules seen in various crustaceans (*32*). In these living animals, deoxygenated hemolymph flows through

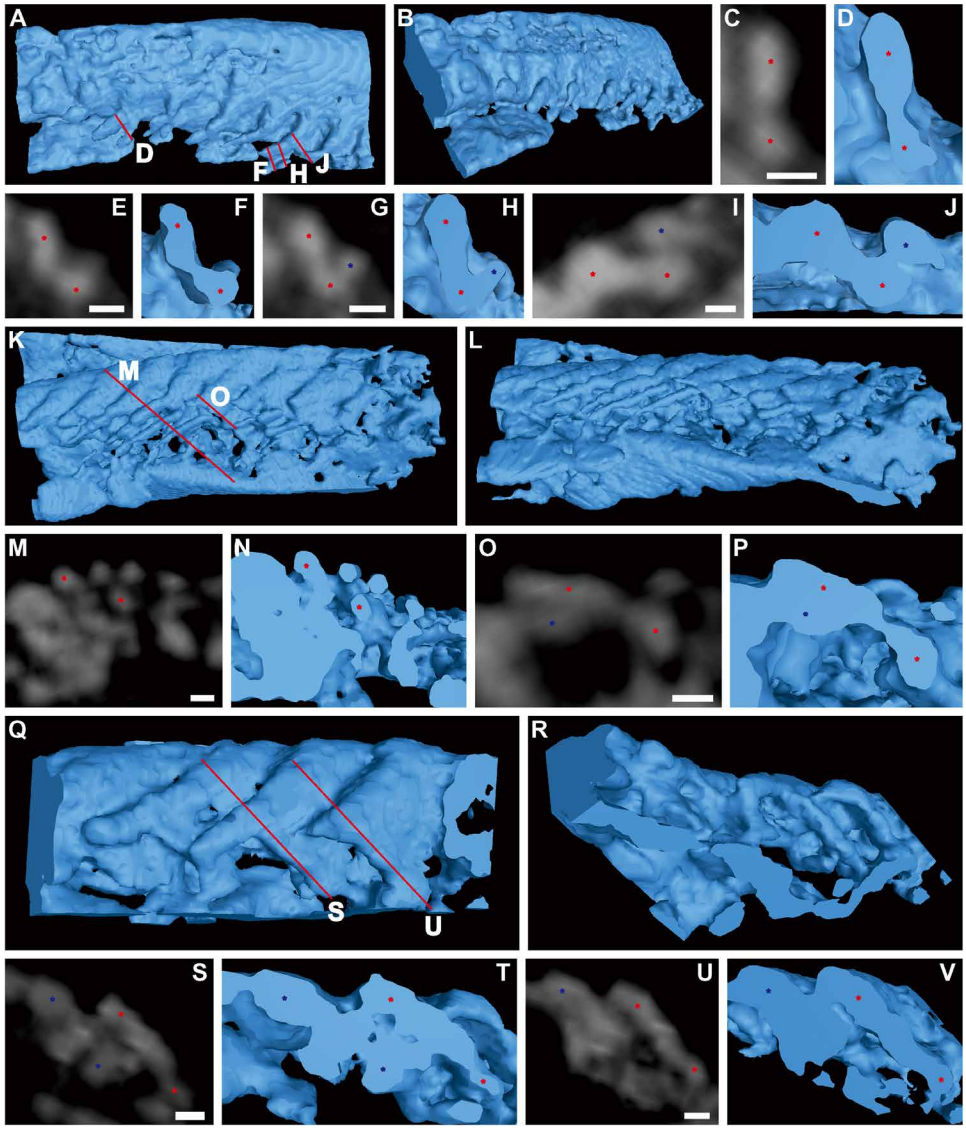

Fig. 2. Dumbbell-shaped filaments of *T. eatoni*. (**A** to **J**) Computed tomography (CT) reconstruction of partial limb, USNM 65527. (A) Dorsal view. (B) Posterolateral view. (C to J) Cross sections of filaments in (A) showing dumbbell-shaped outline with inflated marginal bulbs connected by narrow central region. (**K** to **V**) CT reconstruction of partial limb, USNM 65523. (K) Dorsal view. (L) Posterolateral view. (M to **P**) Cross sections of filaments in (K) showing separately preserved marginal bulbs. (Q) Dorsal view. (R) Posterior view. (S to V) Cross sections of filaments in (Q) show inflated marginal bulbs connected by narrow central region. Asterisks locate the top and bottom inflated marginal bulbs of dumbbell-shaped filaments, which are connected by a narrow central region. CT reconstructions are shown as blue color. CT slices are displayed as gray color. The same color of asterisks represents the same filament. Red lines represent the position of cross sections. Scale bars, 30 μm.

the afferent channel to the tip of the filament, and then, reoxygenated hemolymph flows back through the upper efferent channel of the filament (*33*, *34*) into the body cavity.

The dumbbell-shaped filaments in *T. eatoni* show a notably similar structure, and thus, we infer that they channeled hemolymph in the same way. The afferent channel is suggested to be located at the bottom of the filament and the efferent channel at the top (Fig. 4A). The loop built by both channels permitted bulk flow of hemolymph. The narrow central area of the filament would have been the location for oxygen exchange. The cuticle in this region was likely thin, as it is poorly preserved compared to the robust walls of the bulbs.

Comparable to the filaments in the euarthropods such as trilobites, the setal blades in the lower stem euarthropods, e.g., gilled lobopodians and radiodonts, have also attracted much attention and been widely suggested to have had respiratory function (*19*, *20*, *35*, *36*). These blades are thin and flexible, show rounded termination, and are displayed as fine lamellae (*19*, *20*). In addition, the setal blades, especially in *Opabinia regalis*, attach either on the dorsal surface of the lateral lobe (*37*, *38*) and are suggested to also have a hemocoelic channel (*37*) or to the distal margin of the lateral lobe (*35*). These structures are morphologically and functionally comparable to the filaments of the biramous arthropods, but the lateral lobe to which the blades attached apparently lacked internal muscles. The lateral, gill-bearing lobes in the lower stem euarthropods are considered to be homologous to the upper branch of the biramous fossil arthropods (*37*). Our results further strengthen this argument by establishing

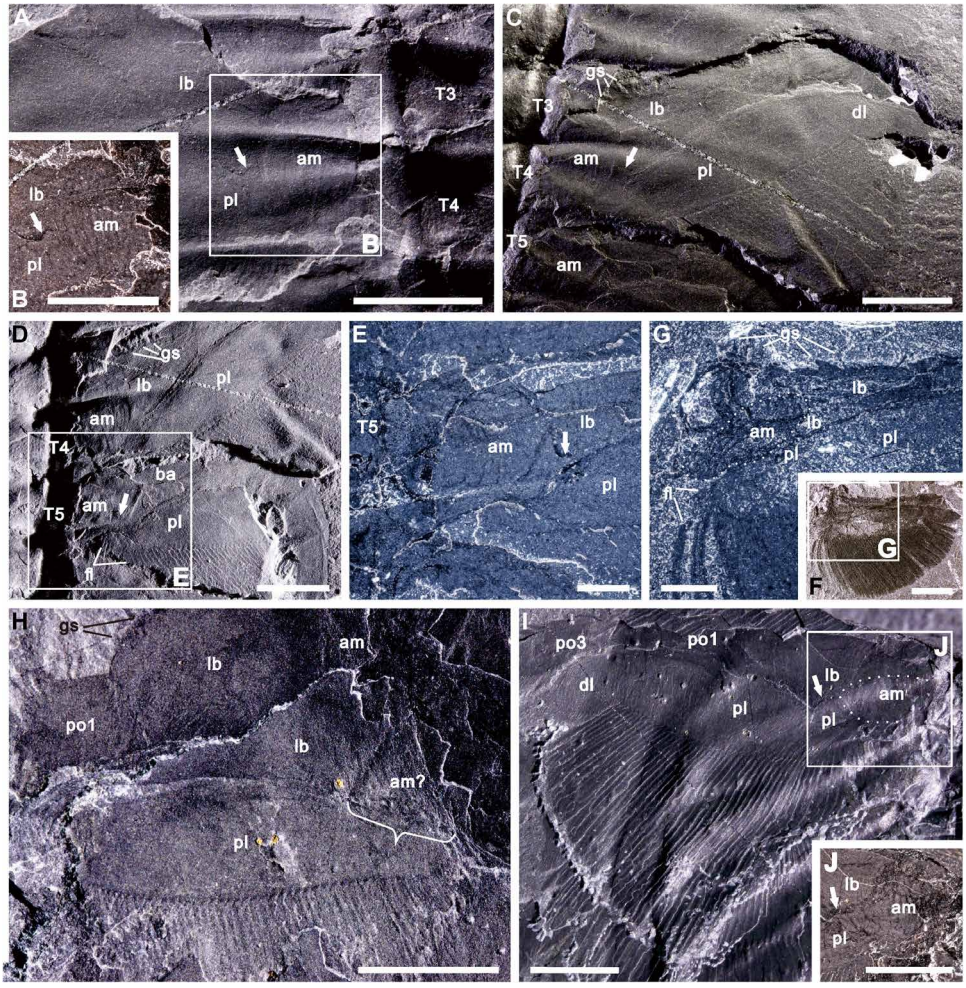

Fig. 3. Articulation of the upper branch of *O. serratus*. (**A** and **B**) Ventral view of USNM 65519 (counterpart) showing upper branch connected directly with wrinkled arthrodial membrane and distinct from limb base. (**C** to **E**) Dorsal view of USNM 65519 (part) showing upper branch connected to wrinkled and convexly arched arthrodial membrane and separated from lower branch. (**F** and **G**) Upper branch connections with the arthrodial membrane and adjacent inner margin of the proximal lobe fringed with filaments extending posteriorly outward, USNM 188574. (**H**) GSC 34692b (part) showing a triangular body-limb junction, of which one side connected with the upper branch (marked by bracket). (**I** and **J**) Both branches articulated with arthrodial membrane, and upper branch clearly separated from lower branch, GSC 34695a (counterpart). (I) Light incident from right. Arrows highlight the boundary between upper branch and limb base. The dotted lines mark the arthrodial membrane outline. Anterior of fossil at top of all images. am, arthrodial membrane; am?, possible arthrodial membrane; gs, gnathobasic spine; dl, distal lobe of upper branch; fl, filament; lb., limb base; pl, proximal lobe; po1 to po3, podomeres 1 to 3, respectively; T3 to T5, thoracic segments 3 to 5, respectively. Scale bars, 5 mm (A to F and H to J) and 2 mm (G).

that the upper limb branch was a gill in *T. eatoni*. The limbs of basal stem Euarthropoda apparently represent an evolutionary stage before the fusion of the respiratory exite and the endopod that became the Paleozoic biramous limb (*19*, *20*).

Articulation of the upper branch

The arrangement of the limb, determined from the posterior flattening of the upper branches in life position, results in minimum overlap between the two branches (fig. S8, A and B). The limb base and upper branch are connected to the body with extended arthrodial membrane (Fig. 3, A to J, and fig. S8, A to C). The connection between the upper branch and the arthrodial membrane shows that the upper branch was not purely an outgrowth of the limb base. The exopod originated either as an entity physically separate from the endopod (Fig. 5A) (*39*) or as an outgrowth of the main posterodistal limb axis (Fig. 5B) (*17*), in which case, it is a second-order structure. Details of the body-limb junction in fossil arthropods are poorly documented (*8*) because the margins of the two branches of the appendage tended to be superimposed during compaction. In *O. serratus*, the upper branch was attached to the inner, posterodorsal edge of the limb base of the lower branch adjacent to the limb-body junction (*40*). The dorsal surface of the limb base is not preserved in this species so that the nature of the limb-body junction is unknown, nor is its position on either the body or the limb base known (*8*). Two possibilities for the articulation of the lower branch and upper branch have been suggested: one, that the upper branch inserted at the distal posterodorsal edge of the limb base (Fig. 6A) (*8*, *40*) in which case, the upper branch articulated purely with the limb base, and two, that the upper branch articulated along the entire posterodorsal edge of the limb base (Fig. 6B) (*41*). However, our

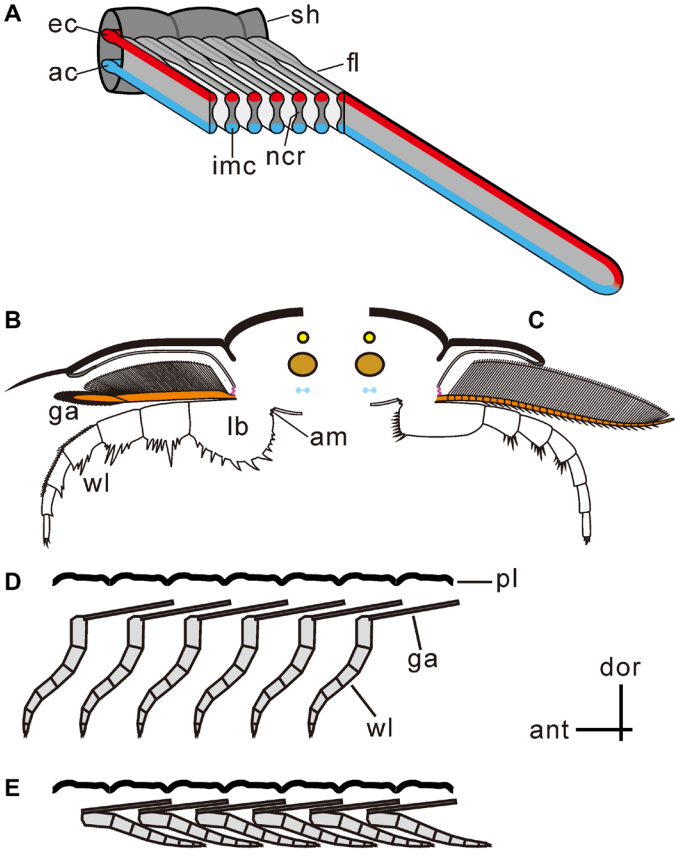

Fig. 4. Reconstructions of trilobite limbs. (**A**) Filaments showing dumbbell-shaped cross section with inflated marginal bulbs and narrow central region, of which the inflated marginal bulbs provide afferent and efferent channels and the narrow central region functioning for respiratory exchange. (**B** and **C**) Cross section showing the upper branch connecting dorsally with the extended arthrodial membrane (purple) and ventrally with the proximal limb base. The upper limb extended posterodorsally, as shown in Fig. 6. (B) Proposed articulation of *O. serratus* [modified from the work of Ramsköld and Edgecombe (*41*)]; anterior view of right limb. (C) Proposed articulation of *T. eatoni* [modified from the work of Whittington and Almond (*57*)]; anterior view of left limb. (**D** and **E**) Imbrication style of two branches limited the movement of the upper branch. (D) Upper branch showing anterior imbrication style, resulting from limited space for limb swinging. (E) Upper branches preserved in anterior imbrication style with lower branches preserved in posterior imbrication style. am, extended arthrodial membrane; ant, anterior; ac, afferent channel; dor, dorsal; ec, efferent channel; fl, filament; ga, gill appendage; imc, inflated marginal channel; lb., limb base; pl, pleura; ncr, narrow central region; sh, shaft; wl, walking leg.

observations show that the upper branch was clearly separate from the limb base in the area in which the upper branch connected with the arthrodial membrane (Fig. 3, A to I, and fig. S8, A to C). This indicates that the upper branch was not connected with the distal posterodorsal edge of the limb base but rather connected with the proximal (or inner) dorsal edge of the limb base. The inner limb margins are usually truncated in fossil specimens (fig. S10 and Supplementary Text), and these truncations contrast distinctly with the sharp outlines of lower branch podomeres. Because of the structural transition between soft and hard tissues, the boundaries of the arthrodial membrane commonly have an irregular margin (Fig. 3, A to I, and fig. S10).

Here, we show that the extended arthrodial membrane pinpoints the location of the limb junction (Fig. 3, A to I, and fig. S8, A to C),

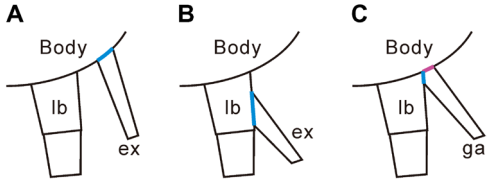

Fig. 5. Reconstructions of arthropod appendages. (**A**) Biramous limb of the Silurian chelicerate *Dibasterium durgae* with the exopod inserted (marked by blue color) separately and independently from the walking leg (*39*). (**B**) Modern arthropodan biramous limb with exopod inserted (marked by blue color) at the limb base of the walking leg (*15*). (**C**) Trilobite limb with gill appendage attached to both limb base ventrally (marked by blue color) and body wall dorsally by extended arthrodial membrane (purple).

which connects the limb to the body. This discounts the idea that the upper branch attached only to the limb base of the lower branch because it was evidently attached both ventrally to the limb base of the lower branch and dorsally to the extended arthrodial membrane (Figs. 5C and 6, C and D). The latter is a thin cuticle stiffened by chitin fibers (*42*) and used to connect rigid body segments, in this case, the scleritized upper limb, to the main body of the trilobite. The book gill of *Limulus* connects with the body in a similar way (*11*) and has been considered as the origin of the epipodite because the gill-bearing potion is located at the proximal limb base rather than the distal limb base where the exopod is typically attached (*11*). Regardless of the origin of the book gill in *Limulus* (*43*), this example is another case in which gill tissue is directly connected with the main body. The close connection between gill tissue and the main body may allow deoxygenated hemolymph to be easily transported to the gill tissues. This articulation might represent the ancestral junction type and imply that in this trilobite, gill tissues were not totally without direct connection to the main body. On the other hand, the articulation of the upper branch in *O. serratus* is also similar to that of the malacostracan arthrobranch gill, except that in malacostracans, the upper branch articulates only along the arthrodial membrane at the junction between the body and the thoracic limb (*18*). The appearance of gill tissues in this particular region in other arthropods shows that the gill structure can be present between the body-limb junction area.

Structural limitations of the upper branches

The upper branch was located between the ventral cuticle of the exoskeletal pleurae and the lower branch (Fig. 4, A and B) (*8*, *40*, *44*), and when viewed from the dorsal side of an animal facing anteriorly, its posterior branches appear to be consistently overlapped by anterior ones (Fig. 4, D and E). The upper branches, characterized by this anterior imbrication style, suggest that the limbs may have been in their natural posture, positioned almost parallel to the plane of the dorsal exoskeleton and also slightly tilted to permit the imbrication observed. This is because the upper branches are distinctly longer extrasagittally than their associated dorsal segments. Movement of the upper branch was apparently limited to the space between the soft tissues adhering to the underside of the dorsal exoskeleton and the lower limb branch beneath it (Fig. 4, D and E) (*44*), and this may have restricted the effectiveness of the limb for swimming. In *O. serratus*, the upper and lower branches are not preserved in an alternating, imbricated series, which might be expected at least occasionally if the upper branch had been able to rotate such that the lamellae were downwardly directed (*40*). The anterior imbrication

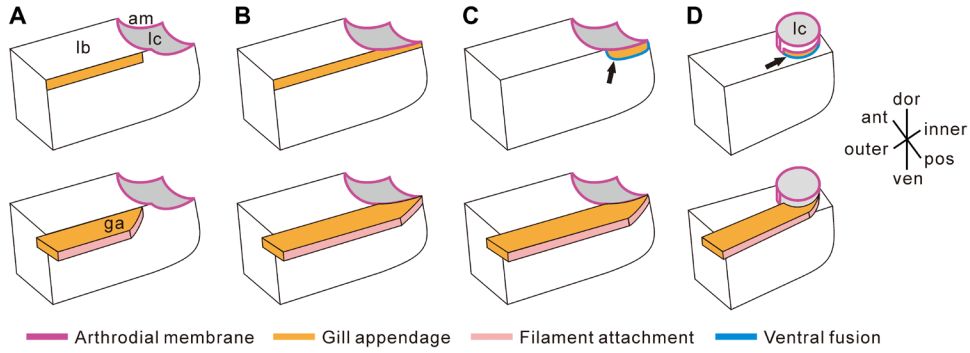

Fig. 6. Articulation of the upper branch. (**A** to **C**) Models of articulation, viewed from posterior of left limb, for *O. serratus*. (A) Upper branch connecting only with the posterior outer portion of the limb base. (B) Upper branch connecting with the full length of the limb base and the extended arthrodial membrane. (C) Our model showing the upper branch attached ventrally to the posterior inner portion of the limb base (indicated by a black arrow) and dorsally to the extended arthrodial membrane. (**D**) Model suggested for *T. eatoni* showing the upper branch connecting ventrally with both the inner portion of the limb base (indicated by a black arrow) and dorsally with the extended arthrodial membrane. The bottom panel shows more complete reconstruction with upper branch in orange; the top panel shows limb base with only the articulation of the upper branch indicated in orange. Blue lines indicated by black arrows show the trilobite upper branch attached to the lower branch ventrally. Purple lines define margin of extended arthrodial membrane with the limb. The pink strip indicates the location of filament insertion. am, extended arthrodial membrane; ant, anterior; dor, dorsal; ga, gill appendage/upper branch; lb, limb base; lc, limb cavity; pos, posterior; ven, ventral.

of the upper branch would result in the majority of adaxial filaments being dorsal to those on more posterior limbs, suspended above the substrate, and thus unlikely to have been used in sediment processing. The posterior imbrication style of the lower limb branches, in which posterior structures cover anterior ones in dorsal view, is much more common in the trunk region, whereas anterior imbrication of the lower branches is more common in the cephalic region. Many early arthropods, such as *M. longicaudata* (*28*, *45*), *Naraoia compacta* (*46*), *Cindarella eucalla* (*25*), and *Xandarella spectaculum* (*28*), display the same condition, with the upper branches showing anterior imbrication, while the lower branches show both anterior and posterior imbrication. This difference may suggest that the cephalic lower branches and trunk lower branches displayed mechanical differences in that the cephalic lower branches tend to rotate forward and the trunk lower branches tend to rotate backward, as is evident in some contemporary arthropod trace fossils (*47*). The contrasting arrangement of the upper (only anterior imbrication) and lower (anterior and posterior imbrication) branches would have limited the range of movement possible for the upper branch. Such a limitation protected the gill filaments and likely allowed aeration but restricted the contribution of the upper branch toward locomotion.

Implications for the comparative biology of arthropod appendages

The underside of the trilobite pleural lobes has been proposed as the logical location for respiratory organs (*11*) because trilobite "exopodal" filaments have been thought to lack structures indicative of respiration (*11*, *12*). Such reasoning also led to the upper branch being considered homologous with the exopod of modern arthropods (*6*, *48*). Here, we have shown that both the physical structure of the dumbbell-shaped filament and its resemblance to known gill lamellae of living mandibulate arthropods (Fig. 4A) indicate that it performed gill function in trilobites. Fusion of the upper and lower branches is similar to that in the malacostracan arthrobranch gill, and the book gill of *Limulus* (Figs. 4B and 5C) in that part of the upper branch is joined directly to the body wall, distinguishing it from the typical junction between the exopod and the limb base. The range of movement of the upper branch may have been relatively limited but sufficient for gill aeration (Fig. 4, D and E). In particular, our interpretations support the idea that movement of the upper branch and lower branch during locomotion would have persistently forced water between the filaments of the upper branch in the animal (*8*). Thus, the evidence presented indicates that the upper branch primarily served a respiratory function (Fig. 4, A to E).

On the basis of its respiratory function and direct junction with the body along part of its length, we suggest that the trilobite upper limb branch may be homologous to the dorsal flap of gilled lobopodians and that both may have shared respiratory function. Attachment of the upper branch or dorsal flap to the body wall characterized basal stem Euarthropoda, e.g., Radiodonta (*19*, *20*), and may have evolved independently in early Chelicerata (*39*) but is distinguished from the typical derived euarthropod exopod that is directly connected only to the protopodite (i.e., basis or coxa). The transition from independent attachment to complete fusion with the limb base has been theorized (*19*, *20*), but evidence of an intermediary stage has not been forthcoming to date. Here, the shared articulation of the upper branch with both the proximal limb base and body wall may represent an intermediate condition before complete merger of two branches in more derived forms. The biramous or dichotomic limb in Trilobita thus may have resulted from the fusion of a walking leg with a respiratory appendage (Fig. 4, B to E). This is consistent with the theory that the limbs of more basal stem Euarthropoda represent an evolutionary stage before the fusion of an exite and the endopod to form the Paleozoic biramous limb (*19*, *20*). Because of the dependence on specific and exceptional preservational modes, our observations on the limb-body junction are currently limited to a single trilobite species, *O. serratus* [the nature of pyrite replacement precludes the preservation of this feature in the *T. eatoni* material examined, but preliminary investigation of the naraoiid *Misszhouia* may suggest a similar style of attachment (see fig. S10 and Supplementary Text)]. New discoveries will be required to determine whether the attachment of the upper limb to both the limb base and the body wall is indeed a trilobite synapomorphy and/or an intermediate state in an evolutionary trend toward complete fusion with the limb base.

The early Paleozoic evolutionary arms race (*49*–*52*) was characterized by increasing exoskeletal regionalization and thicker, more

robust armor with specialized joints. The latter would have limited the effectiveness of a distributed system of cuticular diffusion, which is restricted to small-sized animals (*53*). At larger sizes, increased metabolic demand for oxygen exceeds that provided by cuticular diffusion alone (*54*) and requires specialized respiratory organs, as are apparent in the setal blades of Radiodonta (*19*, *20*, *36*, *37*). Here, we reveal details of gill structure among early arthropods that were acquiring an increasingly reinforced exoskeleton.

MATERIALS AND METHODS

Material described in this paper is housed in the American Museum of Natural History (AMNH), New York, USA; the Geological Survey of Canada (GSC), Ontario, Canada; the Hunterian Museum, University of Glasgow (GLAHM), UK; the National Museum of Natural History (NMNH) of Smithsonian Institution, Washington, DC, USA; and the Yale Peabody Museum of Natural History (YPM), Yale University, USA.

The pyritized specimens of *T. eatoni* are from the Beecher's Trilobite Beds of the Katian (Late Ordovician) Frankfort Shale of upper New York State, USA and the Katian (Late Ordovician) Whetstone Gulf Formation ("Martin Quarry") (*55*, *56*). About 150 specimens of *T. eatoni* were examined, and small, well-preserved ones were selected for environmental scanning electron microscope (ESEM) and micro–computed tomography (μCT) scanning. Specimens of *O. serratus* are from the Burgess Shale biota of the middle Cambrian (Wuliuan stage) Burgess Shale Formation (previously known as the Stephen Formation) of British Columbia, Canada (*4*). About 100 specimens of *O. serratus* were examined. Both species occupied relatively deep shelfal marine environments that may have experienced periodic oxygen availability stress. The specimen of the crab *Cancer* (*Metacarcinus*) *anthonyi* from the west coast of North America was quickly killed with an anatomical scissors.

T. eatoni specimens were scanned with a Phoenix v|tome|x μCT scanner (General Electric Company, Fairfield, CT, USA) at the AMNH Microscopy and Imaging Facility. Postprocessing and volume rendering of the CT images were done using the Phoenix DATOS|x 2 reconstruction software (GE Sensing & Inspection Technologies, Hürth, Germany) and VGStudio MAX version 3.2 (Volume Graphics, Heidelberg, Germany). Tiff image stacks are archived at www.morphosource.org (project P1197).

The specimens were photographed using the Olympus DSX100 Opto-Digital Microscope, Canon EOS 50D, Leica MZ16 with DFC420 lens, Leica M205C with DFC 700T lens, and Philips XL-30 ESEM. The Olympus DSX100 Opto-Digital Microscope and the Leica M205C are installed with stack or nonstack function. ESEM is used with both backscattered electron and gaseous secondary electron technique, which are described in the figures. As specimens are captured with different directions of light to show particular structures, the details are given in the image of the figures. Figures were prepared using CorelDRAW 2018.

SUPPLEMENTARY MATERIALS

Supplementary material for this article is available at http://advances.sciencemag.org/cgi/content/full/7/14/eabe7377/DC1

View/request a protocol for this paper from *Bio-protocol*.

REFERENCES AND NOTES

1. T. W. Lyons, C. T. Reinhard, N. J. Planavsky, The rise of oxygen in Earth's early ocean and atmosphere. *Nature* **506**, 307–315 (2014).
2. M. L. Droser, L. G. Tarhan, J. G. Gehling, The rise of animals in a changing environment: Global ecological innovation in the late Ediacaran. *Annu. Rev. Earth Planet. Sci.* **45**, 593–617 (2017).
3. E. A. Sperling, A. H. Knoll, P. R. Girguis, The ecological physiology of Earth's second oxygen revolution. *Annu. Rev. Ecol. Evol. Syst.* **46**, 215–235 (2015).
4. D. E. G. Briggs, D. H. Erwin, F. J. Collier, *The Fossils of the Burgess Shale* (Smithsonian Institution Press, 1994).
5. J. Yang, J. Ortega-Hernández, N. J. Butterfield, X.-g. Zhang, Specialized appendages in fuxianhuiids and the head organization of early euarthropods. *Nature* **494**, 468–471 (2013).
6. D. Walossek, K. J. Müller, Upper Cambrian stem-lineage crustaceans and their bearing upon the monophyletic origin of Crustacea and the position of *Agnostus*. *Lethaia* **23**, 409–427 (1990).
7. D. J. Siveter, M. D. Sutton, D. E. G. Briggs, D. J. Siveter, An ostracode crustacean with soft parts from the lower Silurian. *Science* **302**, 1749–1751 (2003).
8. H. B. Whittington, Trilobites with appendages from the Middle Cambrian , Burgess Shale, British Columbia. *Fossils Strata*, 97–136 (1975).
9. M. Williams, J. Vannier, L. Corbari, J.-C. Massabuau, Oxygen as a driver of early arthropod micro-benthos evolution. *PLOS ONE* **6**, e28183 (2011).
10. J. Bergström, Remarks on the appendages of trilobites. *Lethaia* **2**, 395–414 (1969).
11. Y. Suzuki, J. Bergström, Respiration in trilobites: A reevaluation. *GFF* **130**, 211–229 (2008).
12. C. Haug, J. T. Haug, New insights into the appendage morphology of the Cambrian trilobite-like arthropod *Naraoia compacta*. *Bull. Geosci.* **91**, 221–227 (2016).
13. C. D. Walcott, The trilobite: New and old evidence relating to its organization. *Bull. Mus. Comp. Zool.* **8**, 191–224 (1881).
14. L. Størmer, Studies on trilobite morphology: The thoracic appendages and their phylogenetic significance. *Norsk Geol. Tidsskr.* **19**, 10–273 (1939).
15. G. A. Boxshall, The evolution of arthropod limbs. *Biol. Rev.* **79**, 253–300 (2004).
16. D. Walossek, K. J. Müller, in *Arthropod Relationships*, R. A. Fortey, R. H. Thomas, Eds. (Springer, 1998), pp. 139–153.
17. C. Wolff, G. Scholtz, The clonal composition of biramous and uniramous arthropod limbs. *Proc. R. Soc. B* **275**, 1023–1028 (2008).
18. G. A. Boxshalll, D. Jaume, Exopodites, epipodites and gills in crustaceans. *Arthropod. Syst. Phylo.* **67**, 229–254 (2009).
19. P. Van Roy, A. C. Daley, D. E. G. Briggs, Anomalocaridid trunk limb homology revealed by a giant filter-feeder with paired flaps. *Nature* **522**, 77–80 (2015).
20. A. C. Daley, G. E. Budd, J.-B. Caron, G. D. Edgecombe, D. Collins, The Burgess Shale anomalocaridid *Hurdia* and its significance for early euarthropod evolution. *Science* **323**, 1597–1600 (2009).
21. R. A. Fortey, Trilobite systematics: The last 75 years. *J. Paleo.* **75**, 1141–1151 (2001).
22. D. E. G. Briggs, R. A. Fortey, The early radiation and relationships of the major arthropod groups. *Science* **246**, 241–243 (1989).
23. M. Stein, G. E. Budd, J. S. Peel, D. A. T. Harper, *Arthroaspis* n. gen., a common element of the Sirius Passet Lagerstätte (Cambrian, North Greenland), sheds light on trilobite ancestry. *BMC Evol. Biol.* **13**, 99 (2013).
24. S. M. Manton, Habits, functional morphology and the evolution of pycnogonids. *Zool. J. Linn. Soc.* **63**, 1–22 (1978).
25. L. Ramsköld, J.-Y. Chen, G. D. Edgecombe, G.-Q. Zhou, *Cindarella* and the arachnate clade Xandarellida (Arthropoda, Early Cambrian) from China. *Trans. R. Soc. Edinb. Earth Sci.* **88**, 19–38 (1997).
26. J. Vannier, C. Aria, R. S. Taylor, J.-B. Caron, *Waptia fieldensis* Walcott,, a mandibulate arthropod from the middle Cambrian Burgess Shale. *R. Soc. Open Sci.* **5**, 172206 (2018).
27. Y. Liu, X.-G. Hou, J. Bergström, Chengjiang arthropod *Leanchoilia illecebrosa* (Hou, 1987) reconsidered. *GFF* **129**, 263–272 (2007).
28. X. G. Hou, J. Bergström, *Arthropods of the Lower Cambrian Chengjiang Fauna, Southwest China*, S. Bengtson, Ed. (Fossils and Strata Series, Scandinavian Univ. Press, 1997), vol. 45, 116 pp.
29. C. M. Luquet, G. A. Rosa, C. C. Ferrari, G. Genovese, G. N. Pellerano, Gill morphology of the intertidal estuarine crab *Chasmagnathus granulatus* Dana, 1851 (Decapoda, Grapsidae) in relation to habitat and respiratory habits. *Crustaceana* **73**, 53–63 (2000).
30. C. A. Astall, S. J. Anderson, A. C. Taylor, R. J. A. Atkinson, Comparative studies of the branchial morphology, gill area and gill ultrastructure of some thalassinidean mud-shrimps (Crustacea: Decapoda: Thalassinidea). *J. Zool.* **241**, 665–688 (1997).
31. J. N. Maina, The morphology of the gills of the freshwater African crab *Potamon niloticus* (Crustacea: Brachyura: Potamonidae): A scanning and transmission electron microscopic study. *J. Zool.* **221**, 499–515 (1990).
32. S. H. Goodman, M. J. Cavey, Organization of a phyllobranchiate gill from the green shore crab *Carcinus maenas* (Crustacea, Decapoda). *Cell Tissue Res.* **260**, 495–505 (1990).
33. C. S. Wirkner, M. Tögel, G. Pass, in *Arthropod Biology and Evolution: Molecules, Development, Morphology*, A. Minelli, G. Boxshall, G. Fusco, Eds. (Springer, 2013), pp. 343–391.

34. J. Le Conte, *Outlines of the Comparative Physiology and Morphology of Animals* (D. Appleton and Company, 1900).
35. X. L. Zhang, D. E. G. Briggs, The nature and significance of the appendages of *Opabinia* from the Middle Cambrian Burgess Shale. *Lethaia* **40**, 161–173 (2007).
36. D. E. G. Briggs, Extraordinary fossils reveal the nature of Cambrian life: A commentary on Whittington (1975)'The enigmatic animal *Opabinia regalis*, Middle Cambrian, Burgess Shale, British Columbia'. *Philos. Trans. R. Soc. B* **370**, 20140313 (2015).
37. G. E. Budd, The morphology of *Opabinia regalis* and the reconstruction of the arthropod stem-group. *Lethaia* **29**, 1–14 (1996).
38. G. E. Budd, A. C. Daley, The lobes and lobopods of *Opabinia regalis* from the middle Cambrian Burgess Shale. *Lethaia* **45**, 83–95 (2012).
39. D. E. G. Briggs, D. J. Siveter, D. J. Siveter, M. D. Sutton, R. J. Garwood, D. Legg, Silurian horseshoe crab illuminates the evolution of arthropod limbs. *Proc. Natl. Acad. Sci. U.S.A.* **109**, 15702–15705 (2012).
40. H. B. Whittington, Exoskeleton, moult stage, appendage morphology, and habits of the Middle Cambrian trilobite *Olenoides serratus*. *Palaeontology* **23**, 171–204 (1980).
41. L. Ramsköld, G. D. Edgecombe, Trilobite appendage structure—*Eoredlichia* reconsidered. *Atcheringa* **20**, 269–276 (1996).
42. H. R. Hepburn, H. D. Chandler, Material properties of arthropod cuticles: The arthrodial membranes. *J. Comp. Physiol. B, Biochem. Syst. Environ. Physiol.* **109**, 177–198 (1976).
43. P. P. Sharma, Chelicerates and the conquest of land: A view of arachnid origins through an evo-devo spyglass. *Integr. Comp. Biol.* **57**, 510–522 (2017).
44. R. R. Hessler, Swimming in crustacea. *Earth Environ. Sci. Trans. R. Soc. Edinb.* **76**, 115–122 (1985).
45. X.-L. Zhang, D.-G. Shu, D. H. Erwin, Cambrian naraoiids (arthropoda): Morphology, ontogeny, systematics, and evolutionary relationships. *J. Paleo.* **81**, 1–52 (2007).
46. H. B. Whittington, The middle Cambrian Trilobite *Naraoia*, Burgess Shale, British Columbia. *Philos. Trans. R. Soc. Lond., B, Biol. Sci.* **280**, 409–443 (1977).
47. A. Seilacher, in *The Geology of Egypt*, R. Said, Ed. (Routledge, 1990), chap. 32, pp. 649–670.
48. D. Walossek, *The Upper Cambrian Rehbachiella and the Phylogeny of Branchiopoda and Crustacea*, S. Bengtson, Ed. (Fossils and Strata Series, Scandinavian Univ. Press, 1993), 202 pp.
49. M. Trestman, The Cambrian explosion and the origins of embodied cognition. *Biol. Theory* **8**, 80–92 (2013).
50. N. C. Hughes, The evolution of trilobite body patterning. *Annu. Rev. Earth Planet. Sci.* **35**, 401–434 (2007).
51. G. D. Edgecombe, D. A. Legg, Origins and early evolution of arthropods. *Palaeontology* **57**, 457–468 (2014).
52. G. J. Vermeij, *Evolution and Escalation: An Ecological History Of Life* (Princeton Univ. Press, 1987), 527 pp.
53. J. B. Graham, Ecological, evolutionary, and physical factors influencing aquatic animal respiration. *Am. Zool.* **30**, 137–146 (1990).
54. P. J. Mill, *Respiration in the Invertebrates* (Macmillan Studies in Comparative Zoology Series, Palgrave, 1972), 212 pp.
55. D. E. G. Briggs, S. H. Bottrell, R. Raiswell, Pyritization of soft-bodied fossils: Beecher's Trilobite Bed, Upper Ordovician, New York State. *Geology* **19**, 1221–1224 (1991).
56. U. C. Farrell, M. J. Martin, J. W. Hagadorn, T. Whiteley, D. E. G. Briggs, Beyond Beecher's Trilobite Bed: Widespread pyritization of soft tissues in the Late Ordovician Taconic foreland basin. *Geology* **37**, 907–910 (2009).
57. H. B. Whittington, J. E. Almond, Appendages and habits of the Upper Ordovician trilobite *Triarthrus eatoni*. *Philos. Trans. R. Soc. Lond., B, Biol. Sci.* **317**, 1–46 (1987).
58. B. Mayers, C. Aria, J. B. Caron, Three new naraoiid species from the Burgess Shale, with a morphometric and phylogenetic reinvestigation of Naraoiidae. *Palaeontology* **62**, 19–50 (2019).
59. A. D. Bond, G. D. Edgecombe, Phylogenetic response of naraoiid arthropods to early–middle Cambrian environmental change. *Palaeontology*, (2020).

Acknowledgments: We thank D. H. Erwin, M. Florence, K. Hollis, F. Marsh, C. C. Labandeira, J. Strotman, and S. Whittaker of NMNH for accessing the specimens and providing research techniques; M. Coyne for assessing specimens of the GSC; D. E. G. Briggs, S. Butts, E. Martin, J. Utrup, and Z. Zhang of YPM for accessing the specimens and research techniques; N. D. L. Clark of GLAHM for access to specimens; M. H. Chase and A. Smith of the AMNH MIF laboratory for technical support; P. Funkhouser for assistance with segmentation; M. L. Droser, E. Casey, and C. Casey for logistic support; and three anonymous reviewers for providing valuable comments that much improved the paper. **Funding:** This research was funded by U.S. NSF EAR-1124303 and EAR-1849963 and the Smithsonian Institution Fellowship Program. It is a contribution to IGCP668. **Author contributions:** J.-b.H. and N.C.H. conceived the project. J.-b.H. and M.J.H. performed research. J.-b.H. and N.C.H. wrote the paper with contributions from M.J.H. M.J.H. processed the computed microtomographic data and made the three-dimensional reconstructions. J.-b.H. photographed specimens with a scanning electron microscope and digital microscopes. J.-b.H. and M.J.H. prepared the plates. **Competing interests:** The authors declare that they have no competing interests. **Data and materials availability:** All data needed to evaluate the conclusions in the paper are present in the paper and/or the Supplementary Materials. Fossil specimens are housed at the AMNH, GSC, GLAHM, NMNH of the Smithsonian Institution, and YPM of Yale University and are available for further research. Additional data related to this paper may be requested from the authors.

Submitted 10 September 2020
Accepted 12 February 2021
Published 31 March 2021
10.1126/sciadv.abe7377

Citation: J.-b. Hou, N. C. Hughes, M. J. Hopkins, The trilobite upper limb branch is a well-developed gill. *Sci. Adv.* **7**, eabe7377 (2021).